Research on Engineering Structures & Materials
www.jresm.org
MIM Research Group

Research Article

Curvature-guarded two-sided Newton and secant bounds for elastic sway buckling of plane frames

Alyaa Abdulrazzaq Azeez [*,1,a], Furat Y. Al-Ghalibi [2,b]

[1]*Ministry of Education, Najaf, Iraq*
[2]*Structures and Water Resources Department, College of Engineering, University of Kufa, Najaf, Iraq*

Article Info

Article History:

Received 19 Oct 2026

Accepted 13 Nov 2026

Keywords:

Elastic critical load;
Sway buckling;
Stability functions;
Two-sided bounds;
Newton's method;
Secant method;
Halley's method;
Portal frame;
Truss

Abstract

Trial-and-error determination of the elastic critical buckling load of symmetric plane frames requires repeated stiffness analyses. Al-Sarraf (1979) proposed estimating this load from one or two trial loads using two criteria—a shear-including criterion (Φ) and a shear-free joint-rotation criterion (Φ_θ)—and interpreting the resulting Newton-type and secant estimates as lower and upper bounds. This study re-examines the method across three benchmark structures from the original paper: a two-story portal frame, a five-story single-bay frame, and a truss. Member stiffnesses are derived from the exact solution of the beam-column equation, and the structures are analyzed using a general exact stiffness method. In the verification analyses, the published stability factors, one-trial bounds, and exact critical load of the two-story frame are reproduced to four significant figures. For the five-story frame, the exact critical load ($\lambda_c = 0.8099$) and multi-trial bounds are confirmed within 0.1% to 0.3% of the published figures. For the truss, the exact load is found to be 1.8793 (a 0.2% difference from the published 1.876), though the original bounds could not be reproduced due to ambiguous half-strut stability-function conventions in the source paper. The findings demonstrate that the two-sided bounding property is not universally valid. A parametric study of 72 single-bay portal frame cases—varying storey counts, stiffness ratios, and trial loads—reveals that the upper estimate can fall below the exact load in multi-story frames, and both estimates can fail near the pole of the no-shear stiffness at the member Euler load. A convexity lemma is presented to explain these behaviors. A proposed curvature test evaluated between the trial load and the Newton estimate proves conservative, ensuring no accepted estimate falls on the wrong side of the exact load across the parametric dataset. Additionally, a Halley-corrected estimator reduces the median error of the lower criterion from 0.53% to 0.07%, though without guaranteeing a strict bound. Ultimately, the results support applying this method to low-rise symmetric frames with moderate stiffness ratios, provided the curvature guard is applied before accepting the estimates as bounds.

© 2026 MIM Research Group. All rights reserved.

1. Introduction

The elastic critical load of a frame governs its stability in the inelastic range. Merchant (1954) proposed it as the basis of an empirical estimate of the carrying capacity of a framework, and Bolton (1955) gave a quick approximation for rigidly jointed trusses that assumes fixed ends for members adjoining the test joint. Both rely on an accurate estimate of the critical load. The exact approach is iterative: the stiffness matrix is assembled at a trial load, its determinant or lowest eigenvalue is computed, and the load is revised until singularity is reached (Livesley and Chandler, 1956; Chen and Lui, 1987). For large frames each analysis is expensive, and bisection to a tolerance of 10^{-6} on

*Corresponding author: dou44444@gmail.com
[a]orcid.org/0009-0002-0236-7538; [b]orcid.org/0000-0001-6244-7965
DOI: http://dx.doi.org/10.17515/resm2026-2495st1019rs

a unit interval requires twenty analyses. Al-Sarraf (1979) proposed to replace this search by one or two analyses. Using stability functions tabulated by Livesley and Chandler, two criteria are formed: a shear-including criterion Φ for the sway mode, and a joint-rotation criterion Φ_θ obtained by considering joint rotations only. Their values and first derivatives at a trial load give Newton estimates, and a pair of trial loads gives secant estimates. The author interpreted the estimates derived from Φ as lower bounds and those derived from Φ_θ as upper bounds on the critical load. The method was demonstrated on three examples, a two-storey portal frame, a five-storey single-bay frame and a truss, using published stability tables.

Modern eigenvalue solvers and general-purpose finite element software evaluate the exact sway load of a frame in a single run, so the motivation for approximate bounds must be stated with care. Approximate bounding methods retain practical value in three settings. In preliminary design, an approximate critical load is sufficient for initial member sizing. In parametric sensitivity studies the critical load must be re-evaluated for many stiffness and section combinations, and a full eigenvalue solution for each combination is wasteful when only the trend is needed. In optimization loops the critical load enters as a constraint and each evaluation should be inexpensive. In such settings a bound that requires one stiffness assembly and one scalar derivative evaluation can be preferable to a full root search, provided that its validity is known in advance rather than assumed. That last condition is the question addressed here: the classical Newton and secant bounds of Al-Sarraf (1979) are examined to establish when they can be relied upon as bounds, and how this can be checked without knowing the exact load. Related studies of the critical load of frames with semi-rigid joints are given by Ihaddoudène et al. (2017, 2018) and buckling finite-element analysis of beams and frames by Bourezane (2012). The review is limited to studies that bear directly on the present formulation and comparison, and it does not claim to cover all later developments. Two claims in Al-Sarraf (1979) need independent verification: that the two estimates bracket the exact critical load, and that the bracket narrows as the trial load approaches it. The first has not been tested beyond the three examples; the second depends on the curvature of the criteria, which the paper does not analyze. The present study addresses both claims with an independent exact implementation. The objectives are: (i) to re-derive the stiffness quantities and reproduce the three published examples; (ii) to identify, numerically and analytically, when the two-sided property holds; (iii) to derive a computable test that flags the estimates which can be used as bounds, without claiming that the test is a proof; (iv) to evaluate a Halley-corrected estimator; and (v) to compare the one-trial, two-trial and exact approaches on a common basis.

The novel elements of the study are the following. An independent exact implementation is used to verify the published values; the root of the joint-rotation criterion is observed to coincide with the exact sway load in all symmetric portal frames examined; a convexity condition is identified that explains when each estimate lies on the correct side of the exact load; a conservative curvature guard is proposed and tested; and the accuracy of a Halley-corrected estimate is assessed. The verification of the published stability factors and examples is not in itself new. The study is restricted to symmetric plane frames with prismatic members and proportional loading by a single load parameter (Section 2.1), and Section 12 discusses the limits.

2. Problem Statement and Notation

2.1 Assumptions and Scope

The frames considered are plane frames whose members are prismatic, with flexural rigidity EI_m and length L_m for member m. Members are treated as axially inextensible. The supports are fixed or pinned. The loading is proportional: a single load parameter λ scales the axial force of every member, so that the axial force of member m is P_m=λ q_m P_(e,m), where P_(e,m)=π^2 EI_m/L_m^2 is the pin-ended Euler load of the member irrespective of its end conditions, and q_m is the reference ratio defined in Section 2.4. Beams carry no axial force, so q_m=0 for beams. The frames are mirror-symmetric, and the critical load is determined from the symmetric (sway) block of the stiffness matrix. The study is restricted to single-bay symmetric frames, for the reason given in Section 4.

2.2 Notation

Table 1 lists the symbols used throughout the paper. Each symbol has one meaning. Scalar criteria are written with the Greek letter Φ, the global stiffness matrix is written in bold, and the sway block carries the subscript s.

Table 1. Symbols used in the paper

Symbol	Meaning
λ	Frame load multiplier
$\lambda_0, \lambda_1, \lambda_2$	Trial loads (Newton: λ_0; secant: $\lambda_1 < \lambda_2$)
λ_c	Exact critical load multiplier (Section 2.3)
$\lambda_{lo}, \lambda_{up}$	Lower and upper estimates of λ_c
$\rho_m = P_m/P_{e,m}$	Load ratio of member m
$P_{e,m} = \pi^2 E I_m/L_m^2$	Pin-ended Euler load of member m
q_m	Reference ratio of member m (Section 2.4)
$K(\lambda)$	Global stiffness matrix after removal of fixed degrees of freedom
$D(\lambda) = detK(\lambda)$	Determinant of the full frame stiffness matrix
$D_s(\lambda)$	Determinant of the symmetric sway block
$\Phi(\lambda)$	Shear-including criterion of Al-Sarraf (1979), $\Phi = A\,\Phi_\theta$
$\Phi_\theta(\lambda)$	Joint-rotation criterion of Al-Sarraf (1979)
$A(\rho)$	Shear-force stiffness factor, $A(0) = 6$
$n(\rho)$	No-shear flexural factor of a member
$g(\rho)$	No-shear carry-over factor of a member
$\kappa = \sqrt{P/EI}$	Wave number of a member
k_{ij}	Entries of the member stiffness matrix k_e
B_{bc}	Boundary-condition matrix of a member (Eq. 6)
r	Beam-to-column stiffness ratio of a single-bay frame
s	Number of stories
$\tau = \lambda_0/\lambda_c$	Trial ratio
$G = \lambda_{up} - \lambda_{lo}$	Gap width between the two estimates

2.3 Definition of the Critical Load

The critical load multiplier λ_c is the smallest positive root of the determinant of the stiffness matrix,

$$D(\lambda)=detK(\lambda)=0 \quad (1)$$

For a mirror-symmetric frame, D factorizes into a symmetric and an antisymmetric block. The sway mode belongs to the symmetric block, in which mirror-image joints have equal rotations and shared horizontal displacements. The critical load is therefore the smallest positive root of D_s (λ)=0, and λ_c always refers to this root. Because q_m=1 for the most heavily loaded member, the load ratio of that member equals the frame load multiplier, ρ_c=λ_c. A single notation λ_c is used for the critical load throughout. Because Newton steps are invariant to a constant factor applied to a function, each criterion may be scaled freely.

2.4 Al-Sarraf's Criteria and Estimates

The reference ratio q_m is obtained from the reference loading of the frame. The ratio of the axial load of each member to its Euler load is evaluated at the reference state and divided by the largest such ratio in the frame, so that $q_m = 1$ for the most heavily loaded member. The ratio may be negative: a truss member in tension has $q_m < 0$. Beams carry no axial force and are assigned $q_m = 0$.

The criteria of Al-Sarraf (1979) are $\Phi(\lambda) = A(\lambda)\,\Phi_\theta(\lambda)$, where A is the shear-force stiffness factor of the most heavily loaded stanchion and Φ_θ is the joint-rotation criterion defined in Section 4. The one-trial estimates are

$$\lambda_{lo} = \lambda_0 - \frac{\Phi(\lambda_0)}{\Phi'(\lambda_0)} \qquad \lambda_{up} = \lambda_0 - \frac{\Phi_\theta(\lambda_0)}{\Phi_\theta{}'(\lambda_0)} \tag{2}$$

and the two-trial secant estimates, with $\lambda_1 < \lambda_2$, are

$$\lambda_{lo} = \lambda_1 + \frac{\lambda_2 - \lambda_1}{1 - \Phi(\lambda_2)/\Phi(\lambda_1)} \qquad \lambda_{up} = \lambda_1 + \frac{\lambda_2 - \lambda_1}{1 - \Phi_\theta(\lambda_2)/\Phi_\theta(\lambda_1)} \tag{3}$$

These are the two-trial expressions of Al-Sarraf (1979), Eqs. (18)–(20) of that paper, written without the sign convention used there.

2.5 Bound and Error Measures

The following measures are used in Sections 6 to 11. An estimate λ_lo is a valid lower bound if λ_lo≤λ_c. An estimate λ_up is a valid upper bound if λ_up≥λ_c. When both hold, the two estimates form a bracket λ_lo≤λ_c≤λ_up. The gap width is G=λ_up-λ_lo. The signed percentage error of an estimate λ_e is 100 (λ_e-λ_c)/λ_c, with a negative value indicating an estimate below the exact load. The trial ratio is τ=λ_0/λ_c, and the parametric study uses τ=0.5, 0.8 and 0.95.

3. Exact Stiffness of a Prismatic Beam-Column with Axial Load

The stability functions of Livesley and Chandler (1956) are commonly quoted in closed form. In this study the member stiffness was derived from the exact solution of the governing equation, which provides an independent check on the published tables. The governing equation of a prismatic member is a standard result of elastic stability theory (Timoshenko and Gere, 1961). For a prismatic member with transverse displacement $v(x)$ under axial force P, equilibrium gives

$$EI\,v'''' + P\,v'' = 0 \tag{4}$$

whose solution, for $P > 0$ *with* $k = \sqrt{P/EI}$*, is*

$$v(x) = C_1 + C_2 x + C_3 sinkx + C_4 coskx \tag{5}$$

The end displacements and rotations $\mathrm{d} = [v_1, \theta_1, v_2, \theta_2]^T$ impose four conditions, $v(0) = v_1$, $v'(0) = \theta_1$, $v(L) = v_2$ and $v'(L) = \theta_2$, which define $\mathrm{A}_{bc}\mathrm{C} = \mathrm{d}$ with

$$A_{bc} = \begin{bmatrix} 1 & 0 & 0 & 1 \\ 0 & 1 & k & 0 \\ 1 & L & sinkL & coskL \\ 0 & 1 & kcoskL & -ksinkL \end{bmatrix} \tag{6}$$

The end actions are the shears and moments of the member, with signs chosen so that the stiffness is symmetric and positive definite at zero load:

$$V_1 = EI\,v'''(0) + P\,v'(0), \quad M_1 = -EI\,v''(0), \quad V_2 = -[EI\,v'''(L) + P\,v'(L)], M_2 = EI\,v''(L) \tag{7}$$

Writing these actions in terms of C gives an operator F and the element stiffness $\mathrm{k}_e = \mathrm{F}\mathrm{A}_{bc}^{-1}$. The ordering of the degrees of freedom is $\mathrm{d} = [v_1, \theta_1, v_2, \theta_2]^T$. For tension ($P < 0$) the same expression is evaluated with a complex square root of P/EI and the real part is retained, which gives continuity across $P = 0$ to machine precision.

Two checks were made on the member matrix. At $P \to 0$ the matrix reduces to the classical element matrix $(EI/L^3)[12,\ 6L,\ -12,\ 6L;\ \ldots]$, so that $k_{12} = 6EI/L^2$ at zero load. For a fixed-free column the lowest root of the free-end block is $P/P_e = 0.25$, the known cantilever result. The classical limits for a single member with the same formulation are the fixed-pinned buckling load $2.046\,P_e$, the fixed-fixed load with sway prevented $4\,P_e$, and the fixed-fixed load with sway permitted P_e (Timoshenko and Gere, 1961). The zero-load matrix and fixed-free cantilever result provide analytical verification checks. The fixed-pinned and fixed-fixed cases give 2.046 and 4.000 times the Euler load, respectively, in agreement with the classical values, obtained as the zeros of the determinant of the boundary-condition matrix.

The shear-force factor is the lateral stiffness of the member with end rotations held at zero. With the normalization $A(0) = 6$ used by Al-Sarraf (1979),

$$A(\rho) = 1/2\ k_{11}(\rho)\ \frac{L^3}{EI} \tag{8}$$

where k_{11} is the (1,1) entry of k_e, that is, the shear force at the near end per unit chord displacement with both end rotations and the far-end translation restrained. By rigid-body translation invariance k_11=-k_13, which was verified numerically: at ρ=0.4, k_11=7.2393 EI/L^3 and k_13=-7.2393 EI/L^3, and the coupling of the near-end translation with the near-end rotation is k_12=5.5936 EI/L^2 at the same load. The chord stiffness is therefore 2A EI/L^3, and the normalization A (0) =6 follows from k_11 (0) =12 EI/L^3.

The no-shear member stiffness is obtained by imposing zero end shear. Because a rigid translation of the member carries no shear, the chord translation is fixed by setting $v_1 = 0$ and solving the shear equation at the far end for v_2. This gives a 2×2 matrix on the end rotations,

$$k_{ns} = \begin{bmatrix} n & -o \\ -o & n \end{bmatrix} \tag{9}$$

where $n(\rho)$ and $g(\rho)$ are the no-shear flexural and carry-over factors of Al-Sarraf (1979). The letter g is used for the carry-over factor so that it is not confused with zero. At $\rho = 0$ both equal 1 EI/L. As ρ approaches the Euler load of the member, n and g become singular (Section 9).

Table 2 compares the computed factors with the values tabulated by Al-Sarraf (1979) at three load levels, and Figure 1 shows the functions over $0 < \rho < 1$. A comparison at no fewer than ten load levels, including the region near $\rho = 1$ and the tension range, would be needed to establish agreement over the full range of the functions. The comparison with Al-Sarraf (1979) is restricted to the load levels listed in Table 2. The available results do not establish agreement throughout the full compression range, near the Euler-load pole, or in tension; conclusions are therefore limited to the tabulated points. The same element is used in a general frame solver. Each member carries its own EI, length, direction and axial load; axial stiffness is taken as $EA = 10^6$ times the bending scale, which represents inextensible members. The element stiffness is transformed to global coordinates and assembled, and the critical load is the first sign change of the determinant of the free-degree-of-freedom matrix. For the joint-rotation criterion, every column contributes its no-shear stiffness and every beam its full rotational block, and the symmetric reduction of Appendix A is applied to both determinants.

Table 2. Stability factors computed in this study compared with the values tabulated by Al-Sarraf (1979)

Factor	ρ	Al-Sarraf (1979)	This study	Difference
A	0.268	4.40782	4.40782	$< 10^{-4}$
A	0.400	3.6197	3.6196	10^{-4}
A	0.526	2.8647	2.8647	$< 10^{-4}$
n	0.400	−0.8781	−0.8781	$< 10^{-4}$
o	0.400	2.1723	2.1723	$< 10^{-4}$

4. Joint-Rotation and Sway Criteria

For the symmetric block, every member is treated as follows. A column contributes its no-shear stiffness k_{ns} on its end rotations, because its ends may translate without shear. This follows from the condition that the transverse force in each column is zero in the sway mode. This holds when three conditions are satisfied: there is no lateral load at the joints, the top story is free, and the frame is single-bay and mirror-symmetric. In a multi-bay frame a zero-story shear does not imply that the shear in every column is zero. In that case condensation must be performed at the structure level rather than member by member. The present study is therefore restricted to single-bay symmetric frames, and this restriction is stated in Section 2.1 and in the title.

A beam that joins two columns contributes its full rotational block, $(EI_b/L_b)\begin{bmatrix}4 & 2\\ 2 & 4\end{bmatrix}$ and with equal end rotations at its two ends this adds $12\,EI_b/L_b$ to the stiffness of the shared joint rotation. The beam's transverse displacement is the vertical displacement of the joints, which is constrained by the axially rigid columns. Under mirror symmetry the rotations of mirror-image joints are equal and the sway is shared.

$$R(\lambda) = \begin{bmatrix} n+6r & -g \\ -g & 2n+6r \end{bmatrix}, \tag{10}$$

For $r = 1$ (the case of Example 1), Eq. (10) reduces to $\Phi_\theta \propto (n+6)(2n+6) - g^2$, which agrees with the expression of Al-Sarraf (1979) once the storeys are ordered and the matrix is scaled. The rotations are ordered with the lower joint first. The constant of proportionality does not affect the zeros of the determinant. The factor of two that appears in the scaling of Al-Sarraf (1979) arises from the two mirror-image columns of each storey, and from the equal-rotation block of the beam.

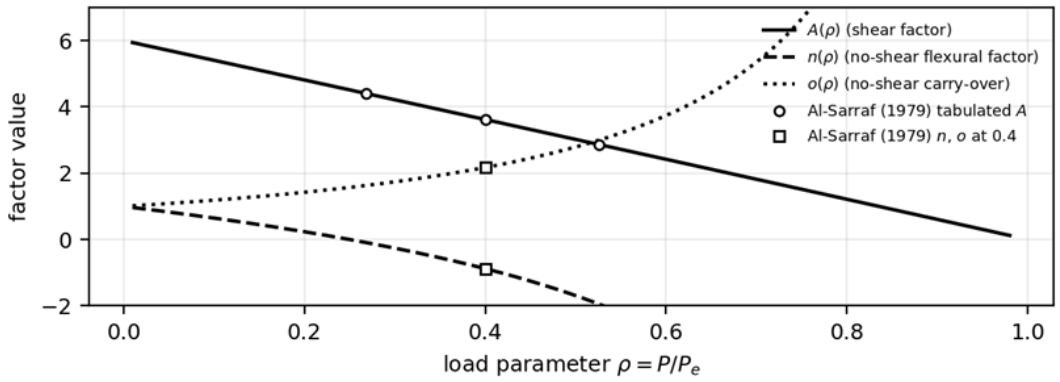


Fig. 1. Stability factors $A(\rho)$, $n(\rho)$ and $o(\rho)$ from the exact member stiffness. Symbols are the tabulated values of Al-Sarraf (1979)

The exact symmetric sway determinant factorizes as

$$D_s(\lambda) = detK_{uu}(\lambda) \cdot \Phi_\theta(\lambda), \qquad \Phi_\theta(\lambda) = det(K_{\theta\theta} - K_{\theta u}K_{uu}^{-1}K_{u\theta}), \tag{11}$$

where K_{uu} is the stiffness matrix of the sway (translational) degrees of freedom, $K_{\theta\theta}$ is the rotational block, and $K_{\theta u}$ and $K_{u\theta}$ are the coupling blocks. The first factor is the determinant of the sway stiffness matrix. The second factor is the determinant of the rotation matrix condensed on the translations, that is, the Schur complement of the translational block. Eq. (11) follows from the block determinant identity, which holds provided K_{uu} is nonsingular (Appendix A). For a single-storey frame K_{uu} is a scalar; for a frame with more than one storey it is a matrix.

The criterion $\Phi = A\,\Phi_\theta$ replaces the factor $detK_{uu}$ of the sway block by the single shear factor A of the most heavily loaded stanchion. This is the approximation on which the lower estimate rests, and its error is examined in Section 9.

5. Bracketing Property of the One-Step Estimates

The following lemma states when a single Newton step bounds the root of a decreasing function from one side.

Lemma 1 (Newton bracketing). Let f be twice continuously differentiable on an interval containing λ_0 and λ_c, with λ_0<λ_c, f>0 on [λ_0,λ_c), f(λ_c)=0 and f'<0. Let λ_1=λ_0-f(λ_0)/f'(λ_0).

- If f″≥0 on the interval between λ_0 and max(λ_1,λ_c), then λ_1≤λ_c.
- If f″≤0 on that interval, then λ_1≥λ_c.

Proof. Let T(λ)=f(λ_0)+f'(λ_0)(λ-λ_0), so T(λ_1)=0. Taylor's theorem with integral remainder gives f(λ)-T(λ)=∫_(λ_0)^λ (λ-s) f″(s) ds, which is nonnegative under (a) and nonpositive under (b) for λ≥λ_0. Under (a), f(λ_1)≥T(λ_1)=0. Since f is decreasing with f(λ_c)=0, f<0 beyond λ_c, so λ_1≤λ_c. Under (b), f(λ_1)≤0, and since f>0 on (λ_0,λ_c), λ_1≥λ_c.

Lemma 1, a one-sided form of the classical bracketing property of Newton's method for monotone convex functions (Ortega and Rheinboldt, 1970), explains the two-sided behavior claimed by Al-Sarraf (1979). A convex lower criterion gives a lower estimate, and a concave joint-rotation criterion gives an upper estimate. The lemma is sufficient and not necessary, and its hypothesis concerns the interval up to the unknown λ_c. Section 9 shows that the hypothesis fails in some multi-story cases, and there the estimate from Φ_θ falls on the wrong side.

An analogous statement holds for the secant estimates. Beyond the trial points, on the side of the root, if the criterion lies above (below) its chord, the chord zero bounds the root from below (above). Because the chord and tangent conditions are verified numerically in the same way, secant and Newton estimates are assessed together in the following sections.

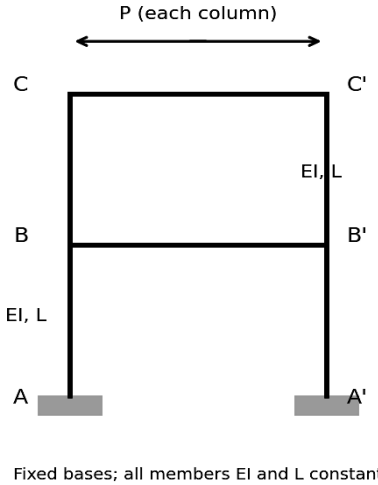


Fig. 2. Two-storey portal frame of Example 1 (Al-Sarraf, 1979). All members have constant EI and L, and each column carries axial load P, shown by vertical arrows. The beams are labeled EI_b and L_b. Geometry and member labels follow Al-Sarraf (1979)

6. Verification on Example 1

Example 1 of Al-Sarraf (1979) is the two-story portal frame of Figure 2 with all members of equal EI and L. Table 3 compares the intermediate quantities and the final estimates from this implementation with the published values and was computed with the general solver of Section 3 applied to the whole frame. The derivatives in the original paper were obtained by differencing tabulated functions with a step of 0.02, and the differences of about 0.05% in K' and $K_\theta{}'$ do not affect the bounds to four decimals.

Table 3. Example 1 of Al-Sarraf (1979) at $\lambda_0 = 0.4$

Quantity	Al-Sarraf (1979)	This study
$A(\lambda_0)$	3.6197	3.6196
$K_\theta(\lambda_0)$	17.0174	17.0178
$K(\lambda_0)$	61.598	61.599
$K'(\lambda_0)$	-549.05	-548.87
$K_\theta{}'(\lambda_0)$	-123.57	-123.51
Lower estimate λ_L	0.5122	0.51223
Upper estimate λ_U	0.5377	0.53778
Exact ρ_c	0.5229	0.52294

The gap between the estimates, $(0.53778 - 0.51223)/0.52294 = 4.9\%$, is the value reported in the original paper. Table 3 shows the dependence on the trial load. The gap closes as $\lambda_0 \to \rho_c$, and the Newton estimate on the exact determinant converges more slowly and is not a bound. Figure 3 shows the normalized criteria for this example. The lower criterion lies below its chord and the upper criterion above it, which is the curvature pattern required by Lemma 1. Figure 4 shows the

Newton iterates from $\lambda_0 = 0.4$. Both sequences reach ρ_c within four iterations, with the lower sequence approaching from below and the upper sequence from above after the first step.

Table 4. Bounds for Example 1 as a function of the trial load

Trial λ_0	Lower λ_L	Upper λ_U	Gap$\lambda_{up} - \lambda_{lo}$	Newton on D
0.20	0.47351	0.61326	0.13975	0.40439
0.30	0.49486	0.56902	0.07416	0.45275
0.40	0.51223	0.53778	0.02555	0.49467
0.45	0.51859	0.52828	0.00968	0.51104
0.50	0.52243	0.52347	0.00105	0.52147
0.52	0.52293	0.52295	0.00002	0.52291

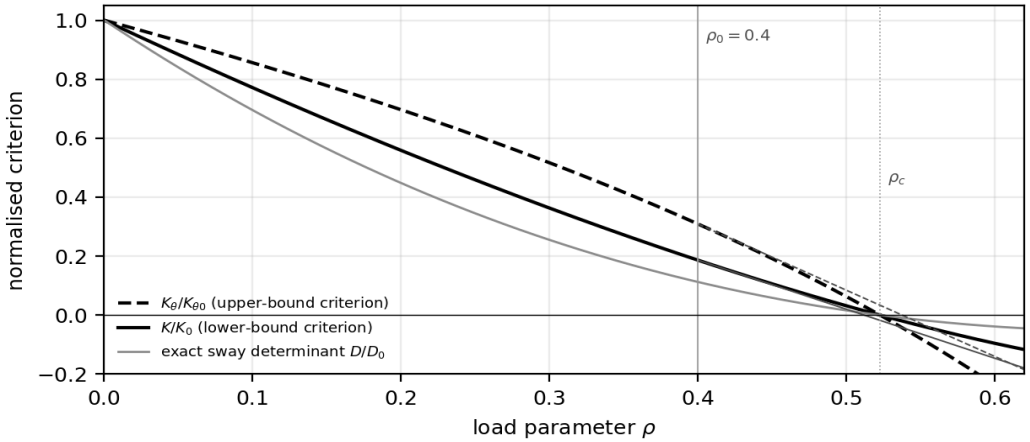


Fig. 3. Normalised criteria for Example 1, with the exact determinant shown for reference. The tangents at $\lambda_0 = 0.4$ give the upper (dashed) and lower (solid) Newton estimates

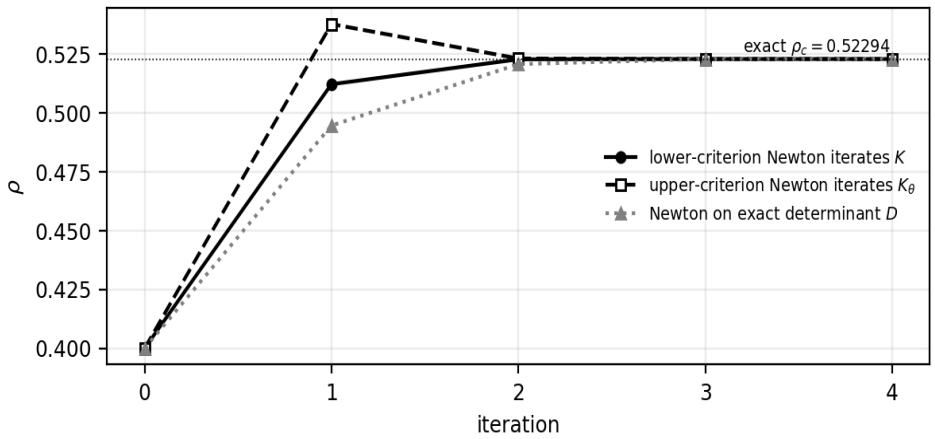


Fig. 4. Newton iterates for Example 1 on K, on K_θ and on the exact determinant D, starting from $\lambda_0 = 0.4$

7. Verification on Example 2

Example 2 of Al-Sarraf (1979) is the five-story single-bay frame of McMinn (1961), with columns of varying length, inertia and load, and beams of length 1.55. The relative properties are those of the source table: column lengths 1.017, 1.050, 0.983, 0.983 and 1.000 (listed from the top story down to the stanchion EF at the base), column inertias 0.277, 0.511, 0.738, 0.902 and 1.000, and reference load ratios q=0.4207,0.7217,0.7274,0.8481 and 1.0000. The beam inertias are 1.579 at the top and 3.936 at the other four levels. The base is fixed and the frame is symmetric. The geometry of Figure 5 follows from the relative lengths.

Solving the symmetric determinant gives $\rho_c = 0.80991$. The published exact value is 0.810, and McMinn's value is 0.81. Figure 6 shows the criteria. The symmetric joint-rotation criterion has the same root as the exact determinant to machine precision, as in Example 1.

Table 5 compares the estimates. A one-trial Newton estimate at the trial $\lambda_0 = 0.526$ used by Al-Sarraf (1979) gives 0.7196 and 0.8517, which bracket the exact load but are wide. The two-trial secant estimates, which the original paper used for this frame because the derivatives of multi-storey criteria are lengthy, agree with the published values to within 0.2% and 0.4% for the first pair and 0.1% for the second. The labels in the original third-trial row appear to be interchanged: the lower estimate is the smaller of the two numbers, as in the present computation.

Table 5. Example 2 of Al-Sarraf (1979): exact load and bounds

Method	Trials	Lower λ_L	Upper λ_U	Published lower / upper	Lower error %	Upper error %
Exact determinant	–	0.80991	0.80991	0.810	–	–
Newton (one trial)	0.526	0.7196	0.8517	–	−11.2%	+5.2%
Secant (two trials)	0.526, 0.7364	0.7763	0.8205	0.7774 / 0.8232	−4.2%	+1.3%
Secant (two trials)	0.7364, 0.789	0.8050	0.8105	0.8114 / 0.8055*	−0.6%	+0.1%

Note: Errors are relative to 0.80991. The published values for the last pair appear with the labels interchanged; read as lower 0.8055 and upper 0.8114, they are consistent with a bracket around 0.8099.

The present secant estimates are 0.1% and 0.3% lower than the published values for the first pair. The difference follows from the shear-free stiffness values, which in the original are read from tables on a coarser load grid. The secant ratios differ by about 2% (0.1593 against 0.1629 for K, and 0.2855 against 0.2921 for K_θ), which is consistent with that source. Halley's estimate, Section 10, improves the one-trial estimates substantially for this frame. At $\lambda_0 = 0.526$ it gives 0.7650 for the lower criterion and 0.8113 for the upper criterion, compared with Newton's 0.7196 and 0.8517.

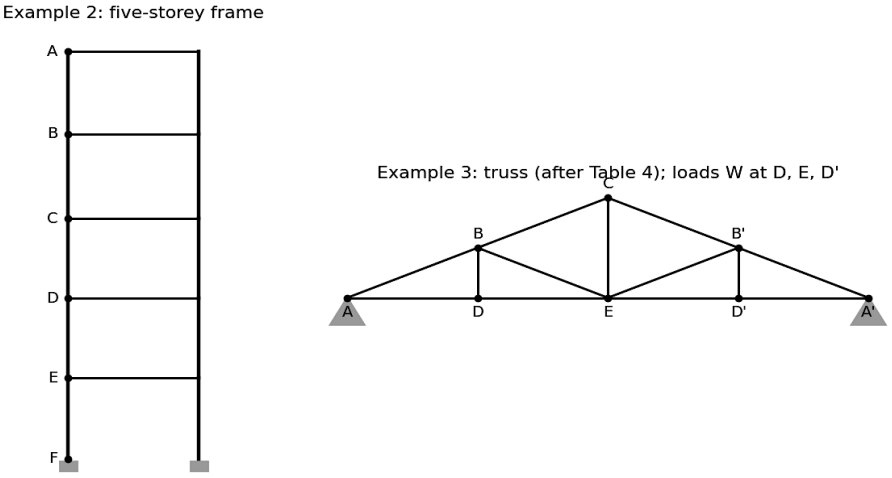


Fig. 5. Geometry of Example 2 (five-storey frame, after McMinn, 1961) and Example 3 (truss, Table 4 of Al-Sarraf, 1979). The truss loads are W at joints D, E and D′

8. Verification on Example 3 (truss)

Example 3 of Al-Sarraf (1979) is a symmetric truss with thirteen members and joints A, B, C, E, D (and their mirror images A′, B′, D′). The relative lengths of Table 4 of the original paper are consistent with the joint coordinates $A(0,0)$, $D(a,0)$, $E(2a,0)$, $D'(3a,0)$, $A'(4a,0)$, $B(a,h)$, $C(2a,c)$ and $B'(3a,h)$ with $a = 0.9285$, $h = 0.3714$ and $c = 0.7428$, which give member lengths of 1.000 for AB, BC and BE, 0.3714 for BD and 0.7428 for CE. The supports at A and A′ are pins. The member

loads are the reference ratios of Table 4 (1.0000, 0.6670, −0.9450, −0.2304, 0.8843 and −1.4114 for the member groups listed there), with negative values denoting tension.

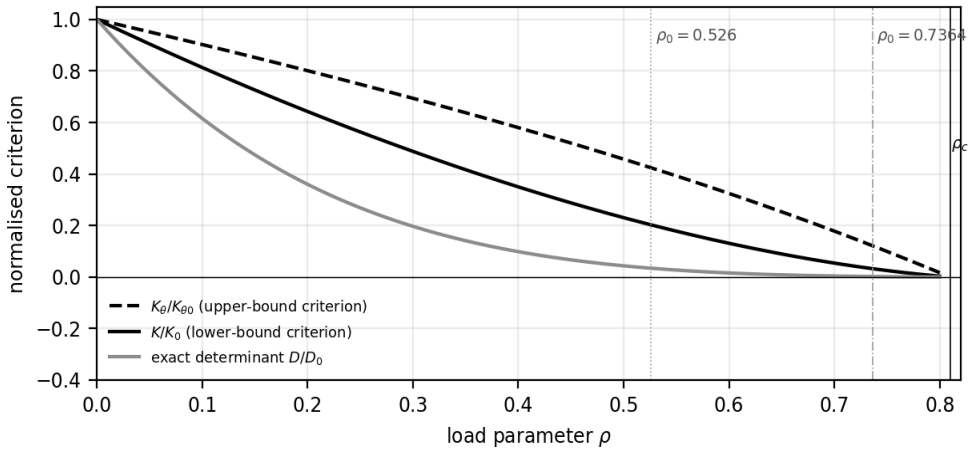


Fig. 6. Normalised criteria for Example 2 with the exact determinant. The root of K_θ coincides with the exact load, and the two trial loads used in Table 4 are marked

The exact critical load of the symmetric block is 1.8793. The published value is 1.876, a difference of 0.2%. Varying the geometry within the precision of the source table changes the root by less than 10^{-4}, so the discrepancy is attributable to the rounding of the tabulated member properties and loads, which could not be isolated further from the published tables. The pinned-support assumption is required: with fixed supports the root is 2.119. The published bounds for this example (Table 6 of the original paper) use a modified Bolton joint-rotation criterion (Eqs. 23–25) with stability functions evaluated for half the most heavily loaded strut, a load parameter of $\rho_{AB}/4$. We implemented the criterion as written in Al-Sarraf (1979), with the joint-rotation Schur complement and the far-joint elimination of Eq. (23), in several variants of the half-strut and symmetry convention. None reproduces the published values. The best variant, using the full strut parameter and a factor of two for mirror pairs in the far-joint terms, gives upper secant estimates of 2.278, 1.907 and 1.860 for the three trial pairs of Table 6, against the published 2.340, 1.906 and 1.875, and lower estimates that differ from the published values for all three pairs. We therefore do not claim a reproduction of the published truss bounds, and Table 6 reports the comparison in full.

Table 6. Example 3 of Al-Sarraf (1979): published bounds, the best reconstruction of the modified Bolton criterion that we obtained, and the exact load

Trial pair (λ_1, λ_2)	Published upper / lower	Reconstruction upper / lower
(0, 1.072)	2.3396 / 1.6793	2.2776 / 1.0320
(1.072, 1.608)	1.9059 / 1.8137	1.9067 / 0.8107
(1.608, 1.876)	1.8745 / 1.8727	1.8595 / 1.8527
Exact	1.8760	1.8793

The exact determinant provides a consistency check on the trusses. For this structure the joint-rotation criterion built from no-shear members on all members does not share the root of the determinant (its root is 0.499), so the approximation of the truss must rely on the far-joint elimination of the modified Bolton form and cannot be replaced by a uniform no-shear treatment. This is a difference from the portal frames, and it is listed as an open question in Section 12.

9. Parametric Study and Failure Modes

9.1 Design

The three benchmarks are not sufficient to test the two-sided property. A parametric study was therefore carried out on single-bay portal frames with one, two and three stories. The columns are identical with $EI_c = L_c = 1$, and the beams have stiffness ratio $r = (EI_b/L_b)/(EI_c/L_c)$ in {0.1,0.25,0.5,1,2,5,20,1000}. Trial loads are 0.5, 0.8 and 0.95 times the exact critical load. This gives

$3 \times 8 \times 3 = 72$ cases of frame and trial load. The exact load was found from the symmetric determinant by scanning for the first sign change and refining with Brent's method to 10^{-14}. First derivatives used central differences with step 10^{-6} and second derivatives used steps of 10^{-4}.

9.2 Principal Results

The first result is that the root of the joint-rotation criterion coincides with the exact sway load. For all 24 frames of Table 7, the root of Φ_θ lies below $\rho = 2$ and agrees with λ_c to within 3×10^{-15} (Figure 9, Section 10.3). The shear-including criterion shares the same root in every frame examined. This is an observed property of the symmetric portal family. It is not proved in general. The second result is that the two-sided property is not general. Table 7 gives the results at $0.8\lambda_c$ for the 24 frames. The lower estimate is valid in 21 of the 24 frames and the upper estimate in 17 of the 24. Over the three trial loads (72 cases) the lower estimate is valid in 63 cases and the upper estimate in 53 cases, and both are valid in 44 cases. At $0.8\lambda_c$ the lower estimate fails only for very stiff beams ($r \geq 20$). The upper estimate fails for two-storey frames with $r \leq 0.25$ (2 of 8 frames) and for three-storey frames with $r \leq 2$ (5 of 8 frames). For three storeys with $r \leq 2$ the upper estimate lies below the exact load while the lower estimate remains valid, so both estimates fall below λ_c. Figure 7 plots the corresponding Newton errors of the lower and upper estimates against the stiffness ratio. The lower/upper validity counts and error statistics in Table 7a were computed from the 24 rows of Table 7 using the definitions in Section 2.5.

Table 7a. Validity counts for the 24 displayed cases at the trial ratio used in Table 7.

Stories	Cases	Lower valid	Upper valid	Both valid	Mean |error| lower / upper (%)
1	8	6	8	6	0.30 / 1,493.24
2	8	7	6	5	1.03 / 496.27
3	8	8	3	3	2.66 / 296.41
Total	24	21	17	14	1.33 / 761.97

Table 7 Parametric results at a trial load of $0.8\rho_c$. A bound is valid if the lower estimate is at most ρ_c or the upper estimate is at least ρ_c. Where K_θ has no root below $\rho = 2$, the exact load is set by the shear factor at $\rho = 1$

n	r	ρ_c (exact)	Root of K_θ	λ_L	λ_U	Lower valid	Upper valid
1	0.1	0.35802	0.35802	0.35655	0.36411	Yes	Yes
1	0.25	0.47915	0.47915	0.47678	0.49330	Yes	Yes
1	0.5	0.61099	0.61099	0.60778	0.64354	Yes	Yes
1	1	0.74766	0.74766	0.74424	0.82694	Yes	Yes
1	2	0.85455	0.85455	0.85189	1.04107	Yes	Yes
1	5	0.93673	0.93673	0.93553	1.46504	Yes	Yes
1	20	0.98354	0.98354	0.98363	3.25087	No	Yes
1	1000	0.99967	none below 2	1.00028	117.13	No	Yes
2	0.1	0.14483	0.14483	0.14368	0.14458	Yes	No
2	0.25	0.24323	0.24323	0.24047	0.24321	Yes	No
2	0.5	0.36525	0.36525	0.36014	0.36728	Yes	Yes
2	1	0.52294	0.52294	0.51479	0.53377	Yes	Yes
2	2	0.68548	0.68548	0.67496	0.72381	Yes	Yes
2	5	0.84729	0.84729	0.83690	0.99055	Yes	Yes
2	20	0.95778	0.95778	0.95267	1.67420	Yes	Yes
2	1000	0.99913	none below 2	0.99959	39.67	No	Yes
3	0.1	0.10121	0.10121	0.09955	0.09993	Yes	No
3	0.25	0.19055	0.19055	0.18569	0.18703	Yes	No
3	0.5	0.30532	0.30532	0.29523	0.29887	Yes	No
3	1	0.46161	0.46161	0.44365	0.45349	Yes	No
3	2	0.63328	0.63328	0.60708	0.63253	Yes	No
3	5	0.81605	0.81605	0.78537	0.86652	Yes	Yes
3	20	0.94805	0.94805	0.92886	1.33198	Yes	Yes
3	1000	0.99993	none below 2	0.99890	23.97	Yes	Yes

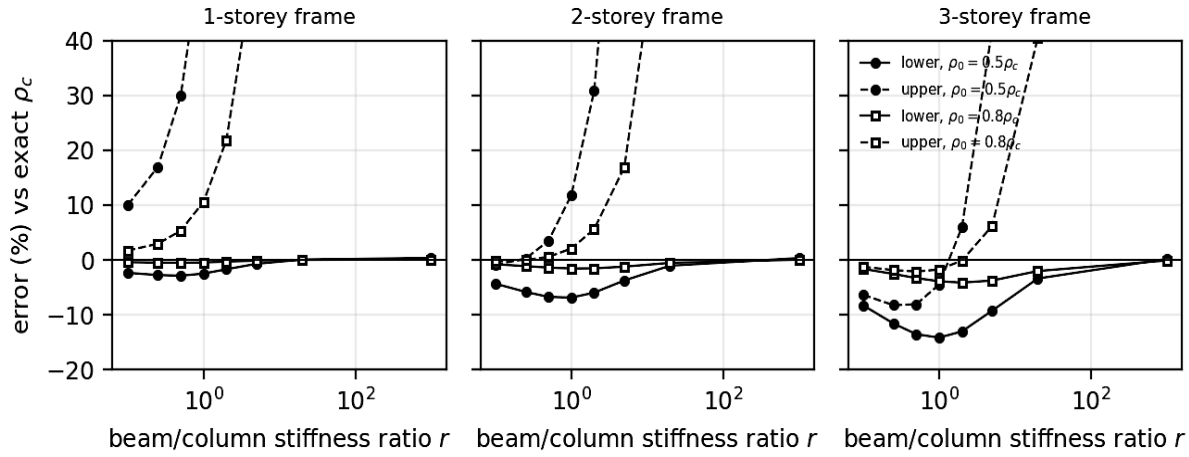


Fig. 7. Error of the lower and upper Newton estimates relative to the exact load for one, two and three storeys, against beam-to-column stiffness ratio. Upper-bound errors above 40% are clipped

The third result concerns the pole at ρ=1. The no-shear stiffness of a member is singular at the member Euler load, where the shear stiffness vanishes and the chord can translate without shear. Near this pole n and g change rapidly, and Φ_θ can acquire a second zero before the pole. The root of Φ_θ lies below ρ=1 in every frame examined, and for r=1000 it lies within (10^{-3}) of the pole, so that a coarse scan can miss the pair of sign changes near the pole. For the two-story frame with r=5, Newton's iteration on Φ_θ from 0.8λ_c overshoots to 0.99055 and converges to 0.97507, where Φ_θ changes sign from negative to positive. This point is not the critical load. Section 10.3 gives the iteration counts.

Two frame-level limits were checked against the parametric values. As $r \to \infty$ the critical load tends to $\rho = 1$: for one, two and three storeys the values at $r = 1000$ are 0.99967, 0.99913 and 0.99892 in Table 7, approaching 1 as the beams become rigid. As $r \to 0$ the beams offer no rotational restraint and, for a single storey, each column behaves as a fixed-free cantilever with $\rho = 0.25$. The single-storey value of 0.35802 at $r = 0.1$ is consistent with a decreasing trend towards this limit, but the limit is not reached in the parametric range. The parameter sweep supports the reported trend over the stiffness ratios actually analyzed. The zero beam-to-column stiffness limit is a theoretical limiting case and has not been numerically established by the parameter sweep reported here; the cantilever interpretation is therefore presented as a limiting argument, not as a completed numerical result.

9.3 Explanation

For one- and two-story frames with moderate stiffness ratios, Φ_θ is concave between the trial load and the critical load, so its estimate is an upper bound, as Lemma 1 predicts. For three storeys with $r \leq 2$, Φ_θ is convex over that interval and its estimate falls below the exact load. The labels "lower" and "upper" are therefore determined by the curvature of each criterion, and they cannot be assigned without checking it. The pole failure arises because Φ_θ varies rapidly as the load approaches 1, and a Newton step from a moderately distant trial load can overshoot into the region of the second zero. In frames with $r \geq 20$ the upper estimate is meaningful only for trial loads below about $0.9\lambda_c$.

10. Curvature Guard and Halley-Corrected Estimator

10.1 Curvature Guard

Lemma 1 requires curvature over an interval containing the exact load, which is unknown. The practical guard therefore uses the interval between the trial load and the Newton estimate. For an upper estimate this interval is the one required by Lemma 1(b), since the upper estimate lies at or beyond the root. For a lower estimate it is shorter than the interval from the trial load to the root required by Lemma 1(a), so the lower-side test is a numerical criterion and not a proof. A lower

estimate is accepted if $\Phi'' \geq 0$ on $[\lambda_0, \lambda_{\text{lo}}]$, and an upper estimate is accepted if $\Phi_\theta'' \leq 0$ on $[\lambda_0, \lambda_{\text{up}}]$. The second derivatives are evaluated by finite differences at five equally spaced points in each interval. Five points give the same acceptance counts as thirty points on the parametric set. With two or three points the number of accepted upper estimates rises to 32 and 26 respectively, so that sign changes of the curvature are missed. Each point requires three evaluations of the scalar criterion. These are evaluations of a 2×2 determinant in n and g, not full frame analyses, and their cost is counted in Table 10. Applied to the 72 cases (24 frames at three trial loads), the guard was evaluated on the valid and invalid estimates as follows. Of the 63 valid lower estimates, 60 were accepted, and the 3 valid lower estimates that were rejected are the conservative cost of the test. All 9 invalid lower estimates were rejected. Of the 53 valid upper estimates, 22 were accepted and 31 were rejected. Of these 31, 24 have $\lambda_{\text{up}} > 1$. Such an estimate lies above the pole, and it is uninformative because the critical load lies below 1 in every frame examined. The guard therefore rejects 7 of the 29 informative valid upper estimates. None of the accepted estimates lay on the wrong side of the exact load. The guard is conservative: it rejects some valid estimates, and this is the price of avoiding invalid ones. Its sufficiency has been verified numerically on the parametric set and is not proved in general.

10.2 Halley-Corrected Estimator

Halley's method (Gander, 1985) corrects the Newton step with curvature:

$$\lambda_H = \lambda_0 - \frac{2f(\lambda_0)f'(\lambda_0)}{2f'(\lambda_0)^2 - f(\lambda_0)f''(\lambda_0)} \tag{11}$$

Over the 72 parametric cases the Halley estimate of the lower criterion had a mean absolute error of 0.69% and a median of 0.07%, against 2.19% and 0.53% for Newton. For the upper criterion the Halley estimate had a mean of 1.31% and a median of 0.19%, against a Newton median of 5.46%; the Newton mean is dominated by near-rigid cases and is not representative. Halley's estimate is not a guaranteed bound: it lay above the exact load in 4 of 72 lower estimates and below it in 29 of 72 upper estimates. We recommend it as a refined approximation, with Newton's estimates and the guard used when a bound is required.

Table 8. Accuracy of one-trial estimates over the parametric set at $\lambda_0 \in \{0.5, 0.8, 0.95\}\rho_c$ (72 cases)

Estimate	Mean abs. error (%)	Median abs. error (%)	Maximum abs. error (%)	Violations of bound
Newton, lower	2.19	0.53	14.17	9
Halley, lower	0.69	0.07	6.35	4 (above exact)
Newton, upper	1653.5*	5.46	63244.9*	19
Halley, upper	1.31	0.19	8.43	29 (below exact)

Note: The Newton upper-criterion mean and maximum are dominated by near-rigid cases ($r = 1000$) and are not representative.

Table 9 gives the Halley estimates for Example 2, which is the main practical case, and Figure 8 shows the error for the two-story frame as a function of trial load. The Halley estimates for Example 2, which is the main practical case, are given in Section 7 and summarized in Table 10 (Section 11), and Figure 8 shows the error for the two-story frame as a function of trial load.

10.3 Iteration Counts

Newton iterations on Φ and on Φ_θ were started from $0.8\lambda_c$ and stopped when the step size $|\lambda_{k+1} - \lambda_k|$ fell below 10^{-8}. Table 9 lists ten selected cases. Over all 24 frames, Newton iteration on Φ converged to λ_c in every case, in three to six steps (median four). Newton iteration on Φ_θ converged to λ_c in 15 of the 24 frames, in three to seven steps (median five). In the remaining nine frames, all with stiff beams ($r \geq 2$ for one storey, $r \geq 5$ for two storeys and $r \geq 20$ for three storeys), the iterates cross the pole and settle on a spurious zero of Φ_θ beyond it. For example, the iteration for the two-storey frame with $r = 5$ converges to 0.97507 instead of $\lambda_c = 0.84729$, and for the one-storey frame with $r = 1000$ it stops at 3.2×10^4 after 70 steps. The step-size test therefore does not guarantee convergence to the critical load for Φ_θ, and a Newton iteration on Φ_θ

should not be used as a root finder without checking the result. Each Newton step requires one evaluation of the criterion and its derivative, so the four to seven steps of the successful cases compare with the twenty full analyses of bisection (Section 11).

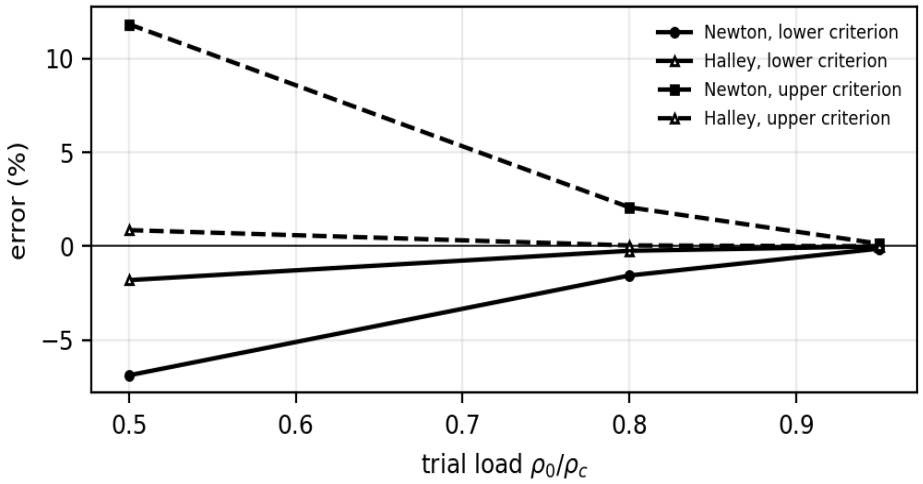


Fig. 8. Error of Newton and Halley estimates for the two-storey frame with $r = 1$, as a function of trial load

Table 9. Newton iteration counts from $0.8\lambda_c$ with stopping tolerance 10^{-8} on the step size. Marked rows converge to a spurious zero of the upper criterion rather than to the critical load; the other failing frames are listed in Section 10.3

Frame	Criterion	Iterations	Converged to	Exact λ_c
1-storey, $r = 1$	Φ	4	0.74766	0.74766
1-storey, $r = 1$	Φ_θ	6	0.74766	0.74766
2-storey, $r = 1$	Φ	4	0.52294	0.52294
2-storey, $r = 1$	Φ_θ	5	0.52294	0.52294
2-storey, $r = 5$	Φ	5	0.84729	0.84729
2-storey, $r = 5$	Φ_θ	9 (pole crossed, converged to second root)	0.97507	0.84729
3-storey, $r = 1$	Φ	5	0.46161	0.46161
3-storey, $r = 1$	Φ_θ	5	0.46161	0.46161
3-storey, $r = 5$	Φ	6	0.81605	0.81605
3-storey, $r = 5$	Φ_θ	7	0.81605	0.81605

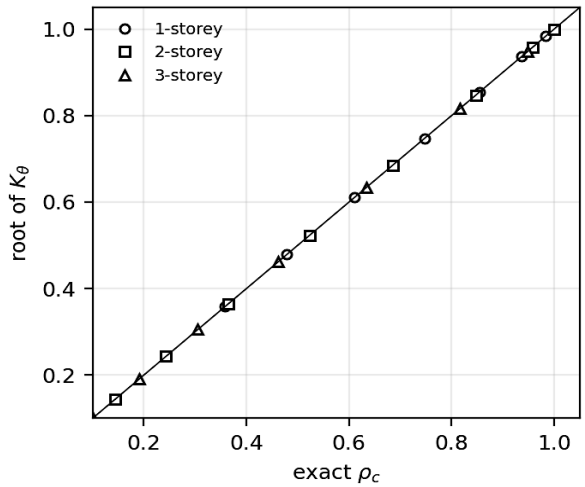


Fig. 9. Root of the joint-rotation criterion against the exact sway load for every frame with a root below $\rho = 2$. All points lie on the identity line to within 3×10^{-15}

11. Comparison of the Methods

Table 10 compares the approaches on the three benchmarks. The cost is counted as the number of stiffness-matrix analyses, with the cost of the scalar criterion evaluations stated separately. The one-trial method requires one analysis of the frame at the trial load, together with the derivatives of the two criteria, which for hand computation are read from tables. The curvature guard of Section 10.1 adds fifteen evaluations of the scalar criterion, which are not analyses. The two-trial method requires two analyses. Bisection to a tolerance of 10^{-6} on [0,1] requires twenty analyses.

Table 10. Comparison of methods on the three benchmarks. Errors are relative to the exact load of each example

Method	Analyses	Example 1 (0.52294)	Example 2 (0.80991)	Example 3 (1.8793)
Newton, one trial (Al-Sarraf)	1 + derivatives	$\lambda_0 = 0.4$: 0.51223 (-2.0%), 0.53778 ($+2.8\%$)	$\lambda_0 = 0.526$: 0.7196 (-11.2%), 0.8517 ($+5.2\%$)	not applicable in the form given
Secant, two trials	2	0.40,0.50: 0.52062 (-0.4%), 0.52577 ($+0.5\%$)	0.526,0.7364: 0.7763 (-4.2%), 0.8205 ($+1.3\%$)	reconstruction, (1.608,1.876) upper 1.860 (-1.0%)
Halley, one trial	1 + second derivative	$\lambda_0 = 0.4$: 0.52108 (-0.4%) for K, 0.52334 ($+0.1\%$) for K_θ	$\lambda_0 = 0.526$: 0.7650 (-5.5%), 0.8113 ($+0.2\%$)	not computed
Exact determinant, bisection	about 20	0.52294	0.80991	1.8793

The comparison shows that a single trial gives a useful bracket for low-rise frames, and that its width depends on how far the trial load is from the critical load. A second trial improves the bracket for multi-story frames at the cost of one further analysis. Halley's correction gives a much tighter estimate with one analysis plus a second derivative, but the estimate is not a bound. For design checks that require an upper bound on the critical load, the curvature guard should be applied, and the exact determinant should be used when the guard rejects the estimate.

12. Discussion and Limitations

The verification shows that the stability factors, the joint-rotation criterion and the one-trial estimates of Al-Sarraf (1979) are reproduced for Example 1. The exact critical load of Example 2 and the two-trial lower and upper estimates of Example 2 are reproduced to within the precision of the source tables. The exact load of Example 3 agrees with the published value to 0.2%. The published truss bounds of Example 3 were not reproduced, and the modified Bolton criterion of that example requires a convention for half-strut stability functions and mirror factors that the original text does not state unambiguously. The conclusions are subject to several limits. Newton iteration on $\Phi_{\theta} $ is not a reliable root finder for stiff beams (Section 10.3), so the joint-rotation criterion is used here only for the one-step estimate and the curvature test. The study considers single-bay symmetric plane frames with prismatic members, fixed or pinned supports, and a single load parameter applied in fixed proportion to the member Euler loads. Multi-bay frames are excluded, because the zero-shear condition on which the no-shear columns rest does not hold there at the member level (Section 4). Semi-rigid connections, non-proportional loading, inclined members in multi-story frames and imperfections are not examined. The symmetric reduction assumes a mirror-symmetric sway mode. The exact loads were computed with the same stiffness formulation as the criteria, not with an independent finite-element eigenvalue analysis. The agreement with the published exact values of Examples 1 and 2 supports the formulation, but it is not a fully independent check. An independent finite-element eigenvalue comparison is

required and is listed as the first next step. The truss treatment is an approximation of an unresolved convention. The curvature guard is conservative and has been verified numerically only. The statement that the root of the joint-rotation criterion coincides with the exact sway load is an observation on the symmetric portal family and is not a general theorem.

13. Conclusions

Al-Sarraf's two-sided method was re-derived from the exact member stiffness and examined on its benchmark frames. The objectives set in Section 1 are assessed as follows. Objective (i), the re-derivation and reproduction of the examples, is fully met for the stiffness quantities and for the portal frames of Examples 1 and 2. It is only partially met for Example 3: the truss bounds could not be reproduced owing to an unresolved stability-function convention, although the exact truss load agrees with the published value of 1.876 to 0.2%. Objective (ii), the identification of when the two-sided property holds, is met numerically. The property holds under a curvature condition, which is explained by the convexity lemma (Lemma 1). The condition fails for taller frames at some stiffness ratios and for trial loads close to the pole at $\boldsymbol{\rho} = \mathbf{1}$. A general proof is not given. Objective (iii), the computable test, is partially met. The curvature guard is computable from the trial load and the Newton estimate, and on the parametric set no accepted estimate lies on the wrong side of the exact load. It is conservative and is not a proof of a guarantee. Objective (iv), the evaluation of the Halley-corrected estimator, is met. The Halley estimates are substantially more accurate than the Newton estimates in median error, but they are not bounds. Objective (v), the comparison of the one-trial, two-trial and exact approaches on a common basis, is met for the portal frames and not met for the truss, for which no common basis was established because the modified Bolton criterion could not be reproduced.

The original contributions of the study are the independent verification of the published examples, the observation that the joint-rotation root coincides with the exact sway load in the symmetric portal family, the convexity condition and the curvature guard derived from it, and the assessment of Halley-corrected estimates in this context. The next steps are an independent finite-element eigenvalue comparison, extension to asymmetric and semi-rigid frames, and a resolution of the modified Bolton convention for trusses.

Appendix A. Symmetric Reduction

Let T map the reduced coordinates of a mirror-symmetric mode to the full degrees of freedom: the rotations and horizontal displacements of mirror-image joints are equated, centre joints have their rotation and horizontal displacement constrained according to the sign of the mode, and fixed degrees of freedom are removed. The reduced stiffness is $\mathrm{T}^T\mathrm{KT}$. For the portal frames the sway mode corresponds to the choice in which mirror rotations and displacements are equal. The joint-rotation criterion uses the rotational rows of T and the no-shear member stiffness on the columns of Eq. (9).

Proof of Eq. (11). For a block matrix $\begin{bmatrix} \mathrm{P} & \mathrm{Q} \\ \mathrm{R} & \mathrm{S} \end{bmatrix}$ with P nonsingular, $\det = \det\mathrm{P}\,\det(\mathrm{S} - \mathrm{RP}^{-1}\mathrm{Q})$. Taking $\mathrm{P} = \mathrm{K}_{uu}$, $\mathrm{Q} = \mathrm{K}_{u\theta}$, $\mathrm{R} = \mathrm{K}_{\theta u}$ and $\mathrm{S} = \mathrm{K}_{\theta\theta}$ gives Eq. (11). The identity requires K_{uu} to be nonsingular; at a sway root $\det\mathrm{K}_{uu}$ is not zero, so the identity applies to the lowest root of D_s that is not a pole of K_{uu}^{-1}. Member stiffness was computed from the closed-form solution of Section 3, verified against the classical matrix at small load and against the cantilever Euler load. Critical loads were found by scanning the symmetric determinant on a uniform grid of 800 to 4000 points, followed by Brent's method with absolute tolerance 10^{-14}. Axial stiffness was taken as $EA = 10^6$ times the bending stiffness scale to represent inextensible members. The criteria were normalized so that $A(0) = 6$; the normalization does not affect Newton or secant estimates, which depend only on ratios. The second derivatives of the curvature guard (Section 10.1) are evaluated by finite differences at five points in each interval, using the scalar criteria only.

References

[1] Al-Sarraf SZ. Upper and lower bounds of elastic critical loads. The Structural Engineer. 1979;57A(12):415-21.

[2] Bolton A. A quick approximation to the critical load of rigidly jointed trusses. The Structural Engineer. 1955 Mar.

[3] Bourezane M. Buckling finite element analysis of beams and frames. In: Proceedings of the World Congress on Engineering 2012; 2012; London, UK. Vol. 1. p. 178-80.
[4] Chen WF, Lui EM. Structural stability: theory and implementation. New York: Elsevier; 1987.
[5] Gander W. On Halley's iteration method. The American Mathematical Monthly. 1985;92(2):131-4. https://doi.org/10.1080/00029890.1985.11971554
[6] Ihaddoudène ANT, Saidani M, Jaspart JP. Influence of joint rigidity on the elastic buckling load of sway and non-sway steel frames. In: Proceedings of the 12th International Conference on Advances in Steel-Concrete Composite Structures (ASCCS 2018); 2018. https://doi.org/10.4995/ASCCS2018.2018.7085
[7] Ihaddoudène ANT, Saidani M, Jaspart JP. Mechanical model for determining the critical load of plane frames with semi-rigid joints subjected to static loads. Engineering Structures. 2017;145:109-17. https://doi.org/10.1016/j.engstruct.2017.05.005
[8] Livesley RK, Chandler DB. Stability functions for structural frameworks. Manchester: Manchester University Press; 1956.
[9] McMinn SJ. The determination of the critical loads of plane frames. The Structural Engineer. 1961 Jul;221-7.
[10] Merchant W. Failure of rigid jointed frameworks as influenced by stability. The Structural Engineer. 1954 Jul.
[11] Ortega JM, Rheinboldt WC. Iterative solution of nonlinear equations in several variables. New York: Academic Press; 1970.
[12] Przemieniecki JS. Theory of matrix structural analysis. New York: McGraw-Hill; 1968.
[13] Timoshenko SP, Gere JM. Theory of elastic stability. 2nd ed. New York: McGraw-Hill; 1961.